Optimal control approaches for Open Pit planning

Emilio Molina, Pierre Martinon, Héctor Rámirez

Optimal control approaches for Open Pit planning

Emilio Molina[a,b,*], Pierre Martinon[a], Héctor Rámirez[b]

[a] *Sorbonne Université, CNRS, Inria, Laboratoire Jacques-Louis Lions (LJLL), 4 Place Jussieu, 75005 Paris, France*
[b] *Departamento de Ingeniería Matemática and Centro de Modelamiento Matemático (AFB170001 - CNRS IRL2807), Universidad de Chile, Santiago, Chile. Beauchef 851, casilla 170-3 Santiago, Chile*

Abstract

This work tackles the Open Pit planning problem in an optimal control framework. We study the optimality conditions for the so-called continuous formulation using Pontryagin's Maximum Principle, and introduce a new, semi-continuous formulation that can handle the optimization of a 2D mine profile. Numerical simulations are provided for several test cases, including global optimization for the 1D Final Open Pit, and first results for the 2D Sequential Open Pit. Results indicate a good consistency between the different approaches, and with the theoretical optimality conditions.

Keywords: mine planning, optimal control, direct transcription method
2010 MSC: 49K30, 49M25, 90C26

1. Introduction

In long-term planning of mine operation, a common task consists in determining the profile of the total mass of material to be extracted from the site to optimally design an opencast mine. This so-called Final Open Pit problem was introduced in the early works Ref. [1, 2], with a more recent overview in Ref. [3].

The typical approach used to solve this problem is based on a discrete block model of the site, each block having an associated extraction cost and profit

*Corresponding author
Email address: emolina@dim.uchile.cl (Emilio Molina)

value, based on topographical and geological data. Using a graph of block precedence (i.e. order of extraction) allows to take into account slope constraints for the mine stability, and gives rise to large Integer Programming problems, see for instance Ref. [4]. The dynamic programming approach was also investigated in this framework, see e.g. Ref. [5]. Another approach presented in Ref. [6] uses a PDE formulation for time labeling functions.

The present paper follows the continuous approach introduced in Ref. [7] with the reformulation of the Open Pit using a calculus of variation framework, and then in [8] as an optimal control problem. The main contributions of the present work include the analysis of the Final Open Pit with capacity, slope and initial profile constraints, using Pontryagin's Maximum Principle to extend the results previously obtained in Ref. [8]. Then we introduce a new semi-continuous formulation that can handle the Sequential Open Pit problem (i.e. optimization of the mine profile over a sequence of several time-frames) for a 2D space domain. Finally, numerical simulations are provided for both the continuous and semi-continuous approaches, including global optimization for the 1D FOP case, and to our knowledge the first results for the 2D profile optimization as an optimal control problem. The outline of the paper is as follows. After the introduction presenting context, Section II covers the SOP problem statement with the continuous approach, and introduces the semi-continuous formulation. Section III presents the FOP analysis using Pontryagin's Maximum Principle and in particular discusses the control structure in terms of bang, constrained and singular arcs. Section IV present the numerical simulations for three test cases: 1D FOP, 1D SOP and 2D SOP, and is followed by the conclusions.

2. Problem statement

For a given spatial domain Ω, we consider a continuous function $p : \Omega \to \mathbf{R}$ called profile that delimits the shape of the mine pit. The aim is to determine the profile that maximizes the gain from the excavated soil, while respecting some limits for the excavated capacity and maximal slope of the mine. We

recall now the continuous approach for open pit planning, and introduce a new semi-continuous approach that can handle the 2D profile case. Both of these approaches lead to optimal control formulations of the problem.

2.1. Continuous formulation

The key idea in the so-called continuous formulation, originally introduced in [7], is to use the distance (position along the x-axis) as independent variable, which allows to define the mine profile as a function of this new 'time'. Introducing a suitable dynamics for this function, with the associated control function, allows to formulate the open pit planning as an optimal control problem (OCP).

2.1.1. Final open pit planning problems (FOP)

For the 1-dimensional case, the domain $\Omega = [a, b]$ will correspond to the independent variable or 'time' of the optimal control problem. Consider the state variables $P, c : [a, b] \to \mathbb{R}^+$ for the depth profile of the pit and the excavated capacity of the mine. Let us also denote $P_0 \in \mathcal{C}^1 \geq 0$ the initial profile corresponding to the natural shape of the ground. We set the state constraint $P(t) \geq P_0(t), \forall t \in [a, b]$, and the boundary conditions $P(a) = P_0(a), P(b) = P_0(b)$. An additional final condition is that the total excavated capacity is limited, i.e. $c(b) \leq c_{max}$.

We also introduce $\kappa : [a, b] \times \mathbb{R} \to \mathbb{R}^*$ such that $\kappa(t, z)$ is the maximal pit slope at position t and depth z. Instead of the original dynamics $\dot{P} = u$, we choose to use a normalized control $u : [a, b] \to [-1, 1]$ which is a bit simpler than having the mixed state-control constraint $|u(t)| \leq \kappa(t, P(t))$ for the maximal slope. As part of the soil characteristics, we also note $G, E : [a, b] \times \mathbb{R} \to \mathbb{R}$ the densities of gain and effort for excavating at a given position and depth. The optimal control formulation of (FOP) is then as follows:

$$
(FOP)\begin{cases}
\max \displaystyle\int_a^b \int_{P_0(t)}^{P(t)} G(t,z)dzdt & \\
\dot{P}(t) = u(t)\kappa(t,P(t)) & \forall t \in [a,b] \\
\dot{c}(t) = \displaystyle\int_{P_0(t)}^{P(t)} E(t,z)dz & \forall t \in [a,b] \\
u(t) \in [-1,1] & \forall t \in [a,b] \\
P_0(t) - P(t) \leq 0 & \forall t \in [a,b] \\
P(a) = P_0(a),\ P(b) = P_0(b) & \\
c(a) = 0,\ c(b) \leq c_{max} &
\end{cases}
$$

Remark. *In the following we take the basic effort function* $E = \mathbf{1}$*. The gain function* G *is typically defined by interpolation over tabular data, and has to be integrated numerically along the depth* z*.*

2.1.2. Sequential open pit planning (SOP)

We introduce now an extended version of (FOP), in which we want to schedule an extraction program over N consecutive time-frames. This case is quite relevant in mine planning since mining companies divide the digging process into periods for operational purposes. We extend the notations of (FOP) to the multi-frame framework, and note P_i the mine profile at time-frame i, with the associated control u_i, while c_i is the excavated capacity during time-frame i. Each mine profile has to be deeper than the previous one, i.e. the constraint $P \geq P_0$ from (FOP) is generalized as $P_i \geq P_{i-1}, i = 1 \dots N$. The capacity limit c^i_{max} is now enforced at each individual time-frame. Finally, the objective function now takes into account a depreciation rate $\alpha > 0$ over time, with the gains for the more distant time-frames being valued less than for the more immediate time-frames. This new optimal control problem reads as follows

$$
(SOP)\begin{cases}
\max \displaystyle\sum_{i=1}^{N} \int_a^b \int_{P_{i-1}(t)}^{P_i(t)} \frac{G(t,z)}{(1+\alpha)^{t-1}} dz dt & \\
\dot{P}_i(t) = u_i \kappa(t, P_i(t)) & \forall t \in [a,b], \quad i = 1, \ldots, N \\
\dot{c}_i = \displaystyle\int_{P_{i-1}(t)}^{P_i(t)} E(t,z) dz & \forall t \in [a,b], \quad i = 1, \ldots, N \\
u_i(t) \in [-1,1], & \forall t \in [a,b], \quad i = 1, \ldots, N \\
P_{i-1}(t) - P_i(t) \leq 0 & \forall t \in [a,b], \quad i = 1, \ldots, N \\
P_i(a) = P_0(a),\ P_i(b) = P_0(b) & i = 1, \ldots, N \\
c_i(a) = 0,\ c_i(b) \leq c_{max}^i & i = 1, \ldots, N
\end{cases}
$$

Remark. *Note that* (SOP) *with* $N = 1$ *corresponds to* (FOP)*. Numerically, the multi-process* (SOP) *can be reformulated by duplicating the state and control variables (as well as the constraints) for each time-frame. Adding the proper linking constraints between the final and initial conditions of the successive time-frames, we obtain a single process version of* (SOP) *that can be solved by standard methods. The overall problem dimension, however, is higher, therefore computationally expensive methods such as global optimization may be able to handle* (FOP) *but not* (SOP)*, see section 4.*

Remark. *For the discrete (block) formulation, it is known (see for instance Ref. [9] and [10]) that each profile (or 'pit') which is solution of* (SOP) *is not deeper than the optimal pit of* (FOP) *with the same parameters and infinite capacity. A similar result has been obtained for the continuous framework in Ref. [7].*

2.2. Semi continuous formulation for SOP

The main limitation of the continuous approach is that using the independent variable to represent the position in space makes it difficult to handle the 2D profile case, both in terms of dynamics / controls and profile slopes. This is

why we introduce a new approach called the semi-continuous formulation, based on an explicit discretization of the space domain Ω. The mine profile is therefore represented by a finite set of variables at the discretization nodes, as illustrated in Figure 1. Control variables are defined as the excavation effort at each discretization node. Slope constraints are modeled as state constraint linking each node with their neighbors. The independent variable is here standard time, expressed in time-frames such that the final time T is the total number of time-frames. Since SOP is a multi-phase problem, one standard way to formulate it is to normalize the time interval to $[0, 1]$ and duplicate the variables for each time-frame. This approach yields another optimal control formulation of the Sequential Open Pit problem, for which extension from 1D to 2D space domain is rather straightforward, at the cost of an increase in overall problem dimension.

Notations. In the context of the semi-continuous approach, for functions of both space and time such as profile, controls and slopes, we will typically use subscripts for the space discretization node in Ω, and exponents for the time-frame of the multi-phase Sequential Open Pit. For instance, P_i^k will represent the profile depth at node i and time-frame k, and $P^k := (P_i^k), i = 0, \dots, N$ refers to the mine profile at time-frame k. Similarly, U_i^k will denote the digging at node i and time-frame k, with $U^k := (P_i^k), i = 0, \dots, N$ corresponding to the overall excavation effort over the domain Ω at time-frame k. We will also denote by $\int_{P^k}^{P^{k+1}}$ the integral of a function between the two mine profiles at time-frames k and $k + 1$; for 1D profiles this is a 2D integral along x and the depth z, and a 3D integral along x, y, z for 2D profiles.

2.2.1. One dimensional profile space domain

Discrete profile. We discretize the space domain $\Omega = [a, b]$ into N equal intervals of length $\Delta x = \frac{b-a}{N}$, with $N + 1$ discretization nodes (x_i), and note $I = \{0, \dots, N\}$ the set of indices for the nodes. We define the state variables for the profile nodes $(P_i)_{i \in I}$ as functions of time. We also introduce the control variables at each node $(U_i)_{i \in I} \geq 0$, corresponding to the excavation effort, so

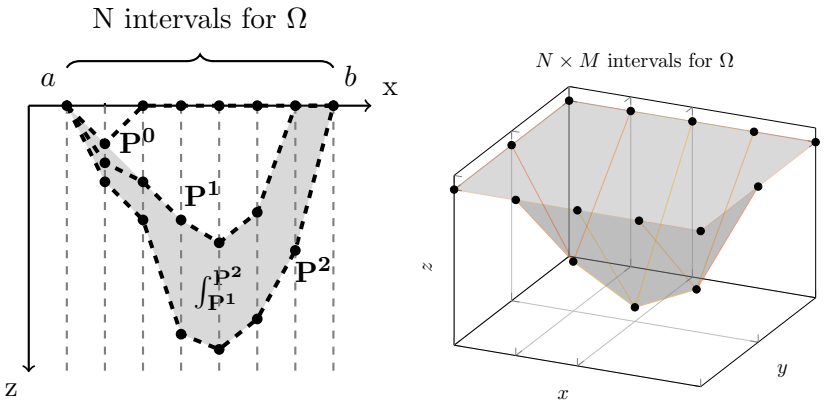

Figure 1: 1D / 2D Space discretization of the mine profile

that the profile variables follow the simple dynamics

$$\dot{P}_i(t) = U_i(t) \ , \ \forall i \in I \ , \ \forall t \in [0, T]. \tag{1}$$

Gain. The gain realized during time-frame k is the integral of G between the current profile P^k and the previous P^{k-1}. Taking into account the depreciation rate α introduced in 2.1.2, the overall gain to be maximized is

$$\sum_{k=1}^{T} \int_{P^{k-1}}^{P^k} \frac{G(x,z)}{(1+\alpha)^{t_k - 1}} dxdz. \tag{2}$$

The computation of this objective is detailed in Appendix A.

Slope. We denote S_i^k the slope at node i and time-frame k, which is a function of time. The maximal slope condition writes as

$$-1 \leq \frac{S_i^k(t)}{\kappa\left(x_i, P_i^k(t)\right)} \leq 1 \ , \ \forall i \in I \ , \ \forall k = 0 \dots T \ , \ \forall t \in [0,1] \tag{3}$$

In the 1D case we will use the simple slope formula

$$S_i^k = (P_i^k - P_{i-1}^k)/\Delta x \tag{4}$$

and the slope limits are state constraints.

125

Capacity. The excavation effort at each time-frame k corresponds to the integral of the effort E between the two consecutive profiles P^{k-1} and P^k, and the capacity limit writes as

$$\int_{P^{k-1}}^{P^k} E(x,z)dxdz \leq C_k, \quad \forall k = 1,\dots,T. \tag{5}$$

The computation of this integral is detailed in Appendix A.

Initial profile. This is now a standard initial condition of the form

$$P_i^0(0) = p_0(x_i)\ ,\ \forall i \in I. \tag{6}$$

We obtain the following multi-phase problem $(SOP)_{SC}^{1D}$ with Fig. 2 illustrating the profile discretization in the 1D case, with $N = 7$ and $T = 2$. Implementation details regarding the approximation of the various integrals are presented in Appendix A

$$(SOP)_{SC}^{1D} \begin{cases} \max \sum_{k=1}^{T} \int_{P^{k-1}}^{P^k} \frac{G}{(1+\alpha)^{k-1}} & \\ \dot{P}_i^k(t) = U_i^k(t) & ,i \in I \quad ,k = 1,\dots,T \quad ,t \in [0,1] \\ -1 \leq \frac{S_i^k(t)}{\kappa(x_i,P_i^k(t)} \leq 1 & ,i \in I \quad ,k = 1,\dots,T \quad ,t \in [0,1] \\ \int_{P^{k-1}}^{P^k} E(x,z)dxdz \leq C_k & ,k = 1,\dots,T \\ P_i^0(0) = p_0(x_i) & ,i \in I \end{cases}$$

Remark. *Setting $T = 1$ corresponds to the Final Open Pit problem with a single time-frame.*

Remark. *The boundary condition $P_{|\partial\Omega} = 0$ is in practice built in directly in the problem formulation by eliminating the profile and control variables at the nodes corresponding to the boundary of the space domain.*

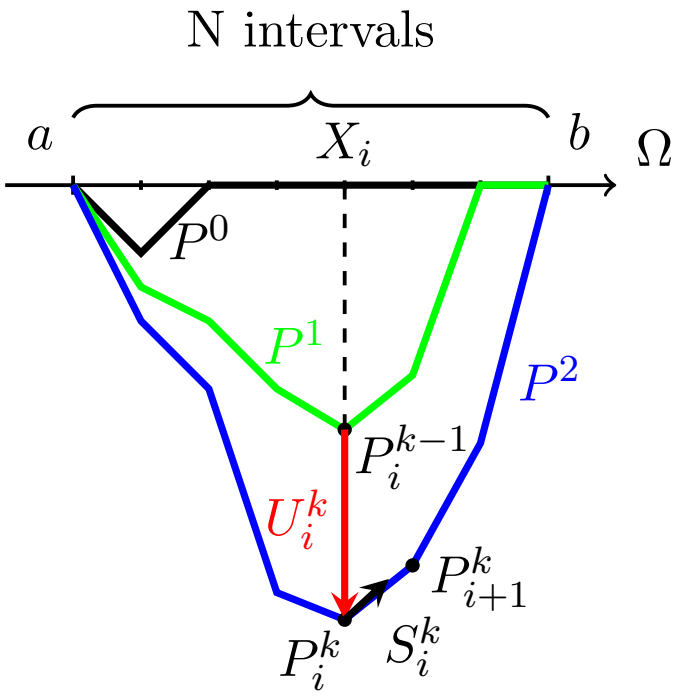

Figure 2: Illustration of the 1D profile model discretized w.r.t. space and time as a set of P_i^k state variables with $i = 0, \dots, N$ profile nodes and $k = 0, \dots, T$ time-frames. Controls U_i^k are the depths excavated from the previous time-frame at each node. Slopes S_i^k between neighbor nodes must be smaller than the local maximal slopes i.e. $\kappa(X_i, P_i^k)$.

Remark. *Moreover, the constraint that each profile must be deeper than the previous one, which was a state constraint in the continuous formulation, is now simply enforced by the conditions* $U_i \geq 0$.

Remark. *The step size* Δx *for the discretization of* Ω *in the semi-continuous approach can be seen as the analogue of the time step* Δt *for the continuous approach, which uses distance as independent variable.*

2.2.2. Two dimensional profile space domain

For the two dimensional case, the extraction domain considered is $\Omega = [a, b] \times [c, d]$. Generalizing the 1D case, we discretize $[a, b]$ and $[c, d]$ into N and

M intervals of length $\Delta x = \frac{b-a}{N}$ and $\Delta y = \frac{d-c}{M}$ respectively, and obtain a grid with $(N+1) \times (M+1)$ nodes. Noting $J = \{0, \ldots, M\}$, we introduce the state variables (functions of time) $(P_{i,j})_{i,j \in I \times J}$ representing the mine depth at each node $(x_i, y_j) := (a + i\Delta x, c + j\Delta y)$. The mine profile at time-frame k is now a surface represented by the set of points $P^k := (P^k_{i,j}(0))$. We introduce the $(N+1) \times (M+1)$ non-negative controls $U^k_{i,j} \geq 0$, $i, j \in I \times J$, with the same dynamics $\dot{P}^k_{i,j} = U^k_{i,j}$.

Initial profile conditions are written as:

$$P^0_{i,j}(0) = p_0(x_i, y_j) \ , \ i, j \in I \times J. \tag{7}$$

The objective and capacity limit are similar to the 1D case, except that the integrals of G and E between two consecutive profiles are now in 3D instead of 2D. The relevant implementation details are provided in Appendix A.

The main adjustment concerns the slope constraint: for each point $P_{i,j}$ of the profile we now choose to consider two slopes $S_{i,j}$ and $T_{i,j}$, in the x-axis and y-axis directions respectively. Using the same basic forward finite differences as in 1D, we obtain the two sets of slope constraints at time-frame k:

$$-1 \leq \frac{P^k_{i+1,j}(t) - P^k_{i,j}(t)}{\kappa\left(x_i, y_j, P^k_{i,j}(t)\right) \Delta x} \leq 1, \quad \forall i = 0, \ldots, N-1, \quad j = 0, \ldots, M-1, \quad \forall t \in [0,1]. \tag{8}$$

$$-1 \leq \frac{P^k_{i,j+1}(t) - P^k_{i,j}(t)}{\kappa\left(x_i, y_j, P^k_{i,j}(t)\right) \Delta y} \leq 1, \quad \forall i = 0, \ldots, N-1, \quad j = 0, \ldots, M-1, \quad \forall t \in [0,1]. \tag{9}$$

Note that more sophisticated choices could be used for the slopes, such as centered differences formulas or increasing the number of slopes considered at each point. The formulation of $(SOP)^{2D}_{SC}$ is summarized below, with Fig. 3 illustrating the profile discretization in the 2D case with $N = 5$ and $M = 3$.

$$
(SOP)^{2D}_{SC}
\begin{cases}
\max \sum_{k=1}^{T} \int_{P^{k-1}}^{P^k} \dfrac{G}{(1+\alpha)^{k-1}} & \\
\dot{P}^k_{i,j}(t) = U^k_{i,j}(t) & ,\forall (i,j) \in I \times J \quad ,k = 1,\dots,T \quad ,t \in [0,1] \\
-1 \leq \frac{S^k_{i,j}(t)}{\kappa\left(x_i, y_j, P^k_{i,j}(t)\right)} \leq 1 & ,\forall (i,j) \in I \times J \quad ,k = 1,\dots,T \quad ,t \in [0,1] \\
-1 \leq \frac{T^k_{i,j}(t)}{\kappa\left(x_i, y_j, P^k_{i,j}(t)\right)} \leq 1 & ,\forall (i,j) \in I \times J \quad ,k = 1,\dots,T \quad ,t \in [0,1] \\
\int_{P^{k-1}}^{P^k} E(x,y,z)dxdydz \leq C_k & ,k = 1,\dots,T \\
P^0_{i,j}(0) = p_0(x_i, y_j) & ,\forall (i,j) \in I \times J
\end{cases}
$$

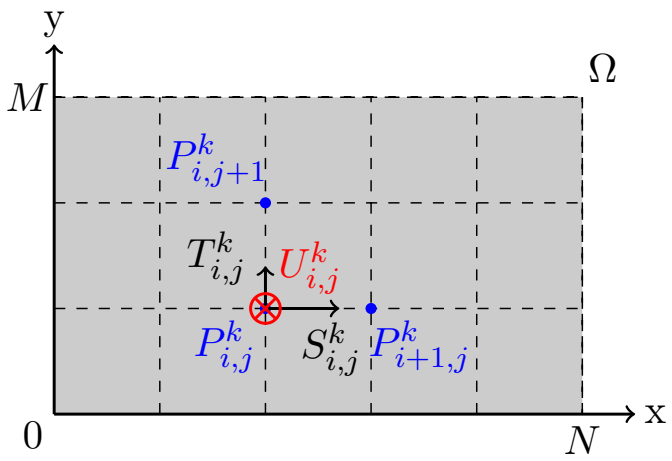

Figure 3: Illustration of the 2D profile model with $N = 5$ and $M = 3$. View is from 'above', with the state variable $P^k_{i,j}$ giving the profile depth at node (x_i, y_j) at time-frame k. Slopes $S^k_{i,j}, T^k_{i,j}$ with neighbors along the x-axis and y-axis must be smaller than the maximal allowed slopes given by the function κ. The control $U^k_{i,j}$ (along the z-axis) corresponds to the excavated depth from the same profile node at the previous time-frame $P^{k-1}_{i,j}$.

3. Analysis and optimality conditions for FOP

We study the final open pit problem in continuous formulation (FOP) by applying Pontryagin's Maximum Principle (Ref. [11]), and look at the possible control structure of optimal profiles.

Optimality conditions for (SOP) are not detailed here, and are more involved in particular due to the state constraint $P \leq P_0$ being generalized over the sequence of time-frames, i.e. $P_i \leq P_{i-1}, i = 1, \ldots, N$.

3.1. Applying Pontryagin's Maximum Principle

Following the formulation in Ref. [12], we now state the PMP for (FOP). We denote y the state variables, p the associated costate variables, l the running cost, f the dynamics and g the state constraint. In all the following we assume the so-called **normal case**, i.e. the multiplier associated to the cost is nonzero and can be normalized to 1. Let us define the pre-Hamiltonian, omitting the argument t of functions u, y, p for clarity:

$$H(t,u,y,p) = l(t,u,y) + p \cdot f(t,y,u) \tag{10}$$

$$= -\int_{P_0(t)}^{P(t)} G(t,z)dz + p_P u\kappa(t,P) + p_c(P(t) - P_0(t)) \tag{11}$$

Noting the function of bounded variation $\mu \in BV(0,T)$ the multiplier associated with the state constraint, the adjoint equation writes as

$$-dP(t) = \nabla_y H(t,u,y,p)dt + \nabla_y g(t,y)d\mu(t) \tag{12}$$

Then for any local optimum $(\bar{y}, \bar{u})$, there exists a non-trivial set of multipliers $(\bar{p}, \bar{\mu})$ such that the following relations are satisfied:

i) Adjoint equation

$$d\bar{p}_P(t) = \left(G(t,\bar{P}) - \bar{p}_P(t)\bar{u}(t)\kappa_P(t,\bar{P}) - \bar{p}_c(t)\right)dt + d\bar{\mu}(t) \tag{13}$$

$$d\bar{p}_c(t) = 0 \tag{14}$$

ii) Transversality conditions

$$\bar{p}_P(a), \bar{p}_P(b), \bar{p}_c(a) \text{ are free; } \bar{p}_c(b) \geq 0 \text{ with } \bar{p}_c(b) = 0 \text{ if } \bar{c}(b) < c_{max} \tag{15}$$

iii) Hamiltonian minimization

$$\bar{u}(t) \in \underset{w}{argmin}\ H(t, w, \bar{y}(t), \bar{p}(t)) \text{ a.e. on } (a, b) \tag{16}$$

iv) State constraint complementary relations

$$d\bar{\mu}(t) \geq 0,\ \int_a^b (P_0(t) - \bar{P}(x))d\bar{\mu}(t) = 0 \text{ and } \bar{\mu}(b) = 0 \tag{17}$$

i.e. $\bar{\mu}$ is an non-decreasing function and is constant when the state constraint is not active.

Remark. *The state constraint is of order* 1 *since the control appears in its first time derivative* $\dot{g} = -u\kappa$. *We refer the reader to, for instance, Ref. [12] for a more in-depth analysis of state constraints in the PMP framework, and especially the so-called "alternate adjoint" formulation.*

3.2. Inactive case: bang/singular control

We start by studying the case when the state constraint is not active. Since per (16) the optimal control minimizes the pre-Hamiltonian which is linear in the control, solutions typically consist in a sequence of **bang** (saturated control) and/or **singular** control arcs. We introduce the **switching function** whose sign will determine the optimal control

$$\psi(t) := H_u(t) = p_P(t)\kappa(t, P(t)) \tag{18}$$

As κ has strictly positive values we obtain the control law:

$$\bar{u}(t) = \begin{cases} 1 & \text{if} \quad p_P(t) < 0 \\ -1 & \text{if} \quad p_P(t) > 0 \\ u_s(t) & \text{if} \quad p_P(t) = 0 \text{ over an interval} \end{cases} \tag{19}$$

The value of the singular control u_s is traditionally determined from the fact that ψ and all its time derivatives vanish over a singular arc.

Over a singular arc, ψ vanishes and the first time derivative of the switching function can be reduced to

$$\dot{\psi}(t) = (G(t, P(t)) - p_c)\kappa(t, P(t)) \tag{20}$$

and similarly, by plugging $\dot{\psi}(t) = 0$ in the second derivative and recalling $\dot{p}_c = 0$, we obtain

$$\ddot{\psi}(t) = (G_t(t, P(t)) + u\kappa G_P(t, P(t)))\kappa \tag{21}$$

Solving $\ddot{\psi}(t) = 0$ for the singular control leads to

$$u_s(t) = -\frac{G_t(t, P(t))}{\kappa G_P(t, P(t))} \tag{22}$$

We can now derive the two following lemmas concerning singular arcs.

Lemma 1. *A singular arc is not admissible when* $|\frac{G_t(t,P)}{\kappa G_P(t,P)}| > 1$*, and in particular when* $G_P(t, P) = 0$*.*

Proof. Immediate consequence of (22) and the control constraint $u \in [-1, 1]$ □

Lemma 2. *Let* $\bar{P}$ *be an optimal profile solution of (FOP), then, over a singular arc the curve* $(t, \bar{P}(t))$ *follows the geodesic of* G*. Moreover, when maximal capacity is not reached, singular arcs follow more specifically the geodesics of null gain* $G = 0$*.*

Proof. From (20), over a singular arc the equation $\dot{\psi} = 0$ indicates that the derivative $\dot{G} := G_t(t, P(t)) + \dot{P}G_P(t, P(t))$ vanishes, therefore the mine profile will follow the geodesics of G. If the maximal capacity constraint is not active, then the associated costate p_c is zero (see (15)), and $\dot{\psi} = 0$ then gives $G = 0$. □

These lemmas expand the analysis of singular arcs obtained in Ref. [8] with calculus of variations techniques.

3.3. Active state constraint case

Over a constrained arc, the control u_c is such that the constraint remains active, i.e. $g = P_0 - P = 0$, leading to the expression

$$u_c(t) = \frac{\dot{P}_0(t)}{\kappa(t, P(t))} \tag{23}$$

Note that a constrained arc can only occur if the u_c is admissible, i.e. $|\dot{P}_0(t)| \leq \kappa(t, P(t))$. This simply means that the initial profile must satisfy the maximal slope constraint.

3.4. Control structure summary

To summarize, the optimal profile, in terms of control structure, is a sequence of bang, singular and/or constrained arcs. **Constrained** arcs are where the profile is the same as the initial one, meaning there was no further excavation on these parts of the domain. **Bang** arcs correspond to the parts of the profile where the slope reaches its maximal allowed value, i.e. the digging is as steep as possible. **Singular** arcs, on the other hand, follow the geodesics of the gain function, meaning the gain is constant along these parts of the profile. Moreover, if the capacity limit is not reached, then this geodesic is more specifically the one of null gain, i.e. the digging stops where excavation is not profitable anymore.

Optimality conditions for **the semi-continuous formulation** are more involved and remain to be investigated thoroughly. The main complications arise from the spatial discretization of the profile, leading to maximal slope limits now being state constraints that involve adjacent nodes variables (including controls).

4. Numerical simulations

We present now the numerical simulations that illustrate the continuous and semi-continuous formulations of the Open Pit problem. After a brief description of the algorithms used for the global and local optimizations, we detail three test cases. First is the 1D FOP with limited capacity, that we solve with the continuous (both global and local optimization) and semi-continuous formulation (local optimization). The second example is the 1D SOP with limited capacity, for which we compare the results of both continuous and semi-continuous formulations (both with local optimization). Finally, we present a test case for the 2D SOP problem with the semi-continuous formulation. All simulations were carried out on a standard laptop, with numerical settings for all methods recalled in Table 1 p.17.

4.1. Numerical methods

4.1.1. Global optimization: FOP with continuous formulation

The Final Open Pit problem is low-dimensional, with only two state variables (not counting the running cost) and one control variable. Therefore it makes sense to try a global optimization method such as dynamic programming, or the so-called Hamilton-Jacobi-Bellman (HJB) approach. We use here the software BocopHJB [13], and refer to for instance Ref. [14] for a detailed description of the HJB method. In this approach the value function of a fully discretized (time, state and control variables) version of the problem is computed, with the global optimum then being reconstructed from this information.

4.1.2. Local optimization: FOP and SOP with continuous and semi-continuous formulations

Since the numerical cost of the global method is too high for the Sequential Open Pit problem, we also use a local optimization method, namely the direct transcription approach. This method approximates the original (OCP) problem by a discretized reformulation as a nonlinear optimization problem (NLP), using a discretization of the time interval. We refer interested readers to for instance Ref. [15] for a review of direct methods. We use here the software Bocop [16], based on the solver Ipopt [17] with sparse derivative computed by the automatic differentiation tool Cppad [18]. This local optimization method is also used for the semi-continuous formulation with explicit discretization of the space domain.

4.1.3. Numerical settings

In Table 1 are the settings for the different numerical methods used in the simulations.

4.2. Final open pit (1D): global and local optimization

We start with the 1D FOP as first example, since it is the only one for which all formulations, including global optimization, are available. We set a

1D FOP (global)	t : 123 steps; P : 50 steps, e : 210 steps; u : 100 steps
1D FOP/SOP (local)	t : 123 steps; $tol = 10^{-10}$; $maxiter = 10000$
1D SOP SC (local)	$t : T$ steps; $N = 123$ nodes; $tol = 10^{-10}$;$maxiter = 10000$
2D SOP SC (local)	$t : T$ steps; 30×10 nodes; $tol = 10^{-6}$;$maxiter = 10000$

Table 1: Numerical settings for the continuous and semi continuous formulations

maximal capacity $c_{max} = 20.000$. The gain function G is interpolated from values found in the Marvin block model of MINELIB, a publicly available library of test problem instances for open pit mining problems (see [19]).

Remark. *Solutions for the unlimited capacity case, with a different control structure (i.e. singular arcs), are shown in Appendix B, with both constant and variable maximal slope.*

4.2.1. 1D FOP with global optimization for continuous approach

The solution obtained by the global optimization is displayed in Figure 4. At first glance, the control structure seems to be of the form **Constrained-Bang-Bang-Constrained**. On both sides the constraint $P = P_0$ is active, meaning there is no additional digging from the initial profile. In the middle, digging occurs with maximal slope, leading to the two bang arcs.

Remark. *The non zero control around $x = 200$ simply follows the existing initial profile P_0, and is part of the first constrained arc. See 4.2.2 for more details.*

Remark. *It is worth noting that an estimate of the PMP costate can be derived from the gradient of the value function computed by the global method, see for instance Refs. [20, 21]. In the present case however, the gradient turns out to be quite noisy and of little practical use. This could be improved by increasing the discretizations, although the increase in computational times would not be competitive with respect to using a direct method.*

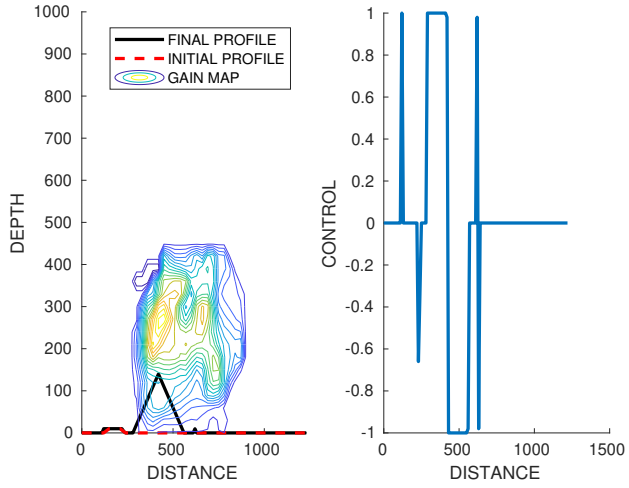

Figure 4: 1D profile with limited capacity - global optimization (HJB method)

4.2.2. 1D FOP with local optimization for continuous approach

The solution from the local optimization is displayed in Figure 5 with the optimal profile and control as well as the PMP costate check. This solution is actually extremely close to the one in section 4.2.1, which indicates that the direct method actually found the global optimum as well, with the benefit of a more accurate solution. In particular, we can here clearly see that the first two arcs with nonzero control around $x = 200$ are not bang arcs since $|u| < 1$: they are actually part of the first constrained arc and correspond to the region where P_0 varies, thus the control $u_c(t) = \frac{\dot{P}_0(t)}{\kappa(t,P(t))}$ from (23) is not just zero.

Moreover, we can now check that the **Constrained-Bang-Bang- Constrained** control structure is consistent with the switching function and the path constraint. We observe a perfect match between the adjoint estimate from the discretized problem and the recomputed PMP costate. Figure 5 shows the value of the state constraint $g = P_0 - P$ and its associated multiplier $d\mu$. We retrieve $d\mu$ from the multiplier of the state constraint in the discretized problem (the correspondence can be inferred from comparing the expression of the PMP Hamiltonian and the Lagrangian of the NLP problem). In accordance with (17),

the multiplier $d\mu$ is positive, and null when the constraint is not active. We also observe that the costate p_P is continuous at the junctions between bang and singular arcs, while the control is discontinuous.

Remark. *In this particular case, the solution has no singular arcs, which is due to the capacity limit that prevents reaching the null gain region. The examples with unlimited capacity in Appendix B and Appendix B.2 illustrate solutions with singular arcs where the optimal profile follows the geodesic* $G = 0$.

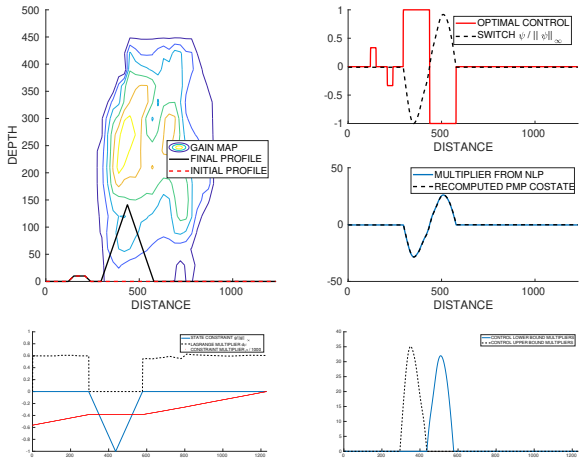

Figure 5: 1D profile with limited capacity - local optimization (direct method) and optimality conditions

4.2.3. 1D FOP with semi-continuous approach

We finally present the solution obtained for the same problem using the semi-continuous formulation with a single phase (i.e $T = 1$). As can be seen in Figure 6 and Table 2, the solution is similar to the global and local optimizations using the continuous approach, with close values for the objective. CPU times are of the same order of magnitude for the two local optimizations with continuous and semi-continuous formulation, while global optimization is significantly slower (two orders).

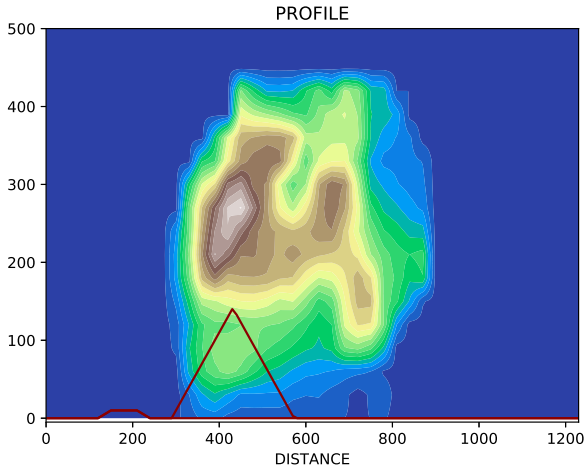

Figure 6: 1D profile, limited capacity - local optimization using semi-continuous formulation

Method	Objective	CPU
1D FOP Global optim.	10846	$369s$
1D FOP Local optim.	11093	$3s$
1D FOP SC Local optim.	11100	$2s$

Table 2: Solutions for the 1D FOP with limited capacity.

4.3. Sequential Open Pit (1D and 2D): local optimization

In this section we present solutions for the Sequential Open Pit. First we solve a 1D example using both the continuous and semi-continuous formulations. Then we show a solution for a more realistic 2D problem using the semi-continuous formulation. To our knowledge, this is the first attempt to tackle the 2D case in an optimal control framework.

4.3.1. 1D SOP with continuous and semi-continuous approach

Continuous approach. We solve the 1D SOP problem for 12 time-frames, with a constant function $\kappa = 1$, a rate $\alpha = 0.1$ and a maximal capacity $c_{max} = 1e4$ for each time-frame. The solution indicates that most of the exca-

vation effort is concentrated in the high gain regions of the domain, which is not surprising.

Semi continuous approach. We now solve the same SOP problem with the semi-continuous formulation. Both approaches give similar solutions, as can be seen in Figure 7. The objective values showed in Table 3 are quite close with a difference of 1.3%, while CPU times are in the same order of magnitude.

Method	Objective	CPU
Continuous	89939	$31s$
Semi-continuous	91153	$43s$

Table 3: Solutions for the 1D SOP problem.

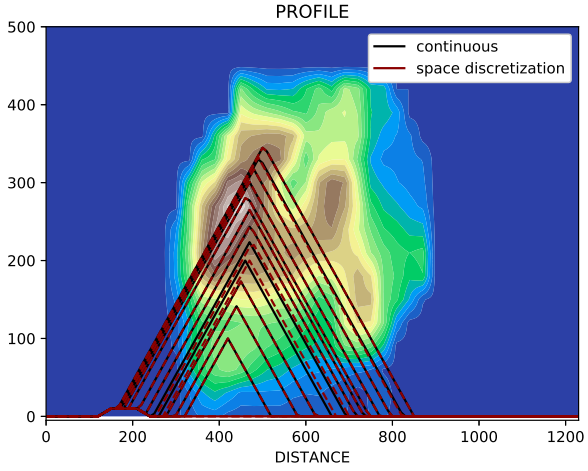

Figure 7: 1D SOP: continuous and semi-continuous formulations.

4.3.2. 2D SOP with semi continuous approach

For the 2D case we consider a domain $\Omega = [0, 1200] \times [0, 400]$ and an analytical gain density function stated by

$$G(x, y, z) = 1000 - \sqrt{(x - 600)^2 + (y - 200)^2 + (z - 350)^2} \tag{24}$$

that reaches its maximal value in $(600, 200, 350)$ and which decreases radially from this point. The initial profile used in this instance is showed in Figure 8.

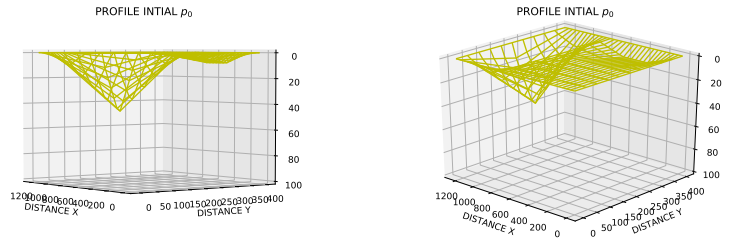

Figure 8: Initial profile for the 2D SOP case

We set a discount factor $\alpha = 0.1$ and solve the 2D SOP for different capacity limits and number of time-frames, using a 30×10 discretization of Ω. Figures 9 and 10 illustrate the optimal sequence of 2D profile corresponding to $c_{max} = 10^6$ and $5 \cdot 10^6$ respectively, with $T = 2, 3, 6$ time-frames. Table 4 shows the objective values and CPU times. Results are consistent overall, with solutions trying to reach the region of highest gain as fast as allowed by the slope and capacity constraints. Increasing the capacity limit and / or the duration of the time interval both yield better objective values, as expected. CPU times are still reasonable, with the longest run at 139s.

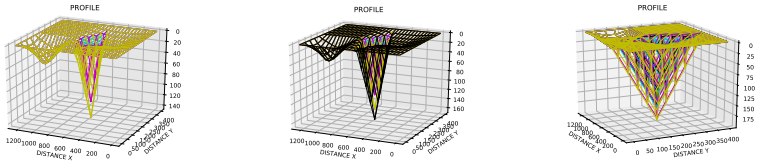

Figure 9: 2D profile optimization with limited capacity $C = 1e6$, for $T = 2, 3$ and 6 time-frames.

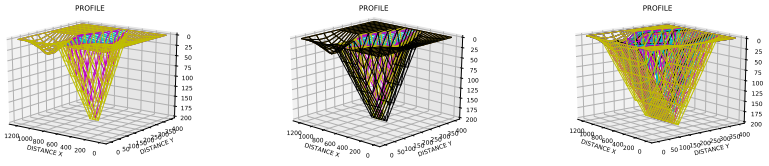

Figure 10: 2D profile optimization with limited capacity $C = 5e6$, for $T = 2, 3$ and 6 time-frames.

	Capacity limit: 10^6		Capacity limit : $5 \cdot 10^6$	
Times-frames	Objective	CPU	Objective	CPU
$T = 2$	69954.88	$11s$	73089.311	$53s$
$T = 3$	100103.04	$38s$	104684.29	$124s$
$T = 6$	175132.64	$31s$	183583.57	$139s$

Table 4: 2D SOP: solutions from the semi-continuous formulation, for different time intervals and capacity limit per time-frame.

5. Conclusions

In the present work we focused on the Open Pit problem in an optimal control framework. We extended some previous results on the optimality conditions for the Final Open Pit, and introduced a new semi-continuous formulation that handles the 2D profile sequential optimization. Numerical simulations are provided for the continuous and semi-continuous approaches on several test cases. The 1D FOP case showed a good consistency between global and local optimization for the continuous approach, as well as local optimization for semi-continuous, and matched the optimality conditions from Pontryagin's Principle. Then the 1D SOP case again indicated a good match for the continuous and semi-continuous formulations. Finally we solved a 2D SOP test case, to our knowledge for the first time in an optimal control framework. Perspectives in the continuation of the present work include solving a more complete 2D SOP example using 3D interpolated data for the gain and maximal slope, as well as studying the optimality conditions for the semi-continuous approach. The

latter could prepare for the use of indirect shooting methods such as HAMPATH [22], especially since the local optimization method used here can provide the knowledge of the optimal control structure and a costate approximation.

6. Acknowledgment

This work was partially supported by ANID-PFCHA/Doctorado Nacional/2018-21180348, FONDECYT grant 1201982 and Centro de Modelamiento Matemático (CMM), ACE210010 and FB210005, BASAL funds for center of excellence, three from ANID (Chile)

References

References

[1] H. Lerchs, G. I., Optimum design of open pit mines, Trans CIM 58 (1965) 47–54.

[2] T. B. Johnson, Optimum open pit mine production scheduling, Tech. Rep. ORC-68-11 (1968).

[3] A. Newman, E. Rubio, R. Caro, A. Weintraub, K. Eurek, A review of operations research in mine planning, Interfaces 40 (3) (2010) 222–245. doi:10.1287/inte.1090.0492.

[4] L. Caccetta, Application of optimisation techniques in open pit mining, Springer, Boston, MA., 2007. doi:10.1007/978-0-387-71815-6_29.

[5] E. A. Wright, The use of dynamic programming for open pit mine design: some practical implications, Mining Science and Technology 4 (2) (1987) 97–104. doi:10.1016/S0167-9031(87)90214-3.

[6] A. Griewank, N. Strogies, A pde constraint formulation of open pit mine planning problems, Proceedings in Applied Mathematics & Mechanics 13 (1) (2013) 391–392. doi:10.1002/pamm.201310191.

[7] F. Alvarez, J. Amaya, A. Griewank, N. Strogies, A continuous framework for open pit mine planning, Mathematical methods of operations research 73 (1) (2011) 29–54. doi:10.1007/s00186-010-0332-3.

[8] J. Amaya, C. Hermosilla, E. Molina, Optimality conditions for the continuous model of the final open pit problem, Optimization Letters (2019) 1–17doi:10.1007/s11590-019-01516-8.

[9] L. Caccetta, S. P. Hill, An application of branch and cut to open pit mine scheduling, Journal of global optimization 27 (2-3) (2003) 349–365. doi:10.1023/A:1024835022186.

[10] E. Molina, J. Amaya, Analytical properties of the feasible and optimal profiles in the binary programming formulation of open pit, in: Application of Computers and Operations Research in the Mineral Industry, Golden, Colorado USA, 2017.

[11] L. Pontryagin, V. Boltyanski, R. Gamkrelidze, E. Michtchenko, The Mathematical Theory of Optimal Processes, Wiley Interscience, New York, 1962.

[12] F. Bonnans, A. Hermant, Revisiting the analysis of optimal control problems with several state constraints, Control Cybernet 38 (4A) (2009) 1021–1052.

[13] F. Bonnans, P. Martinon, D. Giorgi, V. Grelard, S. Maindrault, O. Tissot, Bocop - A collection of examples, Tech. rep., INRIA (2019).
URL http://www.bocop.org

[14] M. Falcone, R. Ferretti, Semi-Lagrangian approximation schemes for linear and Hamilton-Jacobi equations, SIAM, 2013.

[15] J. T. Betts, Practical methods for optimal control using nonlinear programming, Society for Industrial and Applied Mathematics (SIAM), Philadelphia, PA, 2001.

[16] F. Bonnans, P. Martinon, D. Giorgi, V. Grelard, S. Maindrault, O. Tissot, BOCOP - A toolbox for optimal control problems, http://bocop.org (2019).

[17] A. Waechter, L. T. Biegler, On the implementation of an interior-point filter line-search algorithm for large-scale nonlinear programming, Mathematical Programming Series A 106 (2006) 25–57. doi:10.1007/s10107-004-0559-y.

[18] B. M. Bell, CppAD: a package for C++ algorithmic differentiation, Computational Infrastructure for Operations Research.

[19] D. Espinoza, M. Goycoolea, E. Moreno, A. Newman, Minelib: a library of open pit mining problems, Annals of Operations Research 206 (1) (2013) 93–114. doi:10.1007/s10479-012-1258-3.

[20] F. H. Clarke, R. B. Vinter, The relationship between the maximum principle and dynamic programming, SIAM Journal on Control and Optimization 25 (5) (1987) 1291–1311. doi:10.1007/978-1-4612-1466-3_5.

[21] E. Cristiani, P. Martinon, Initialization of the shooting method via the hamilton-jacobi-bellman approach, Journal of Optimization Theory and Applications 146 (2) (2010) 321–346. doi:10.1007/s10957-010-9649-6.

[22] J.-B. Caillau, O. Cots, J. Gergaud, Differential pathfollowing for regular optimal control problems, Optim. Methods Softw. 27 (2) (2012) 177–196.

Appendix A. Implementation details for the semi-continuous approach

Time discretization. The Sequential Open Pit for the semi-continuous approach described in 2.2 is a multi phase problem. Instead of duplicating the variables for each time-frame, we use here in practice a more compact implementation, by using a time step Δt of 1 time-frame, i.e. the time discretization $t_k = 0 \dots T$ is the sequence of time-frames. This choice makes sense from the operational point of view, since the sequential open pit planning precisely consists in determining the optimal mine profile at each time-frame. It also simplifies

a lot the computation of the integrals of the gain and effort functions between two successive mine profiles. We choose an implicit Euler scheme for the time discretization, which gives the trivial discrete dynamics

$$P_i^{k+1} = P_i^k + U_i^{k+1} \tag{A.1}$$

that easily gives the next / previous mine profile when needed in the computations.

Gain. An additional state variable g is added to represent the gain realized along the time-frames, whose dynamics can be written as

$$\dot{g}(t_k) = \frac{1}{(1+\alpha)^{k-1}} \int_{P^{k-1}}^{P^k} G(x,z)dxdz, \quad \forall k = 1, \dots, T \tag{A.2}$$

The objective is then to maximize $g(T)$. For the 1D case, we approximate the 2-dimensional integral of G by trapezoidal rule over x then along z. In the 2D profile case, the 3D integral of G for the computation of the gain is approximated using a 2D trapezoidal rule along (x, y) then a standard trapezoidal rule along z.

Capacity. At each time-frame, the integral of the excavation effort over the domain Ω can be approximated by

$$\int_{P^{k-1}}^{P^k} E(x,z)dxdz \approx \sum_{i=0}^{N} \Delta x \left(\int_{P_i^{k-1}}^{P_i^k} E(x_i,z)dz \right) \tag{A.3}$$

Since $E = 1$ and from the discrete dynamics $P_i^k = P_i^{k-1} + U_i^k$, we can use the following formula

$$\int_{P^{k-1}}^{P^k} E(x,z)dxdz \approx \Delta x \sum_{i=0}^{N-1} U_i^k. \tag{A.4}$$

Similarly, for the 2D profile case, the excavation effort at time-frame k is approximated as

$$\int_{P^{k-1}}^{P^k} E(x,y,z)dxdydz \approx \Delta x \Delta y \sum_{i=0}^{N-1} \sum_{j=0}^{M-1} U_{i,j}^k. \tag{A.5}$$

Appendix B. Additional examples for the final open pit - continuous formulation

Appendix B.1. FOP with infinite capacity and constant slope

We show here the basic example with unconstrained capacity, namely $c_{max} = \infty$. Fig. B.11 shows the solution obtained by the global method, and Fig.B.12 shows the solution from the local method, and we observe that both solutions match. With infinite capacity, the solution, as expected, digs as much as possible with respect to the maximal slope, until it reaches negative gain. This corresponds to the observed **Bang-Singular-Bang** control structure (neglecting the two very small constrained arcs $P = P_0 = 0$ at the extremities). As stated in Lemma 2, the singular arc in the middle follows the geodesic $G = 0$. The corresponding control also matches the theoretical expression of the singular control (19), despite some oscillations at the junctions with the bang arcs.

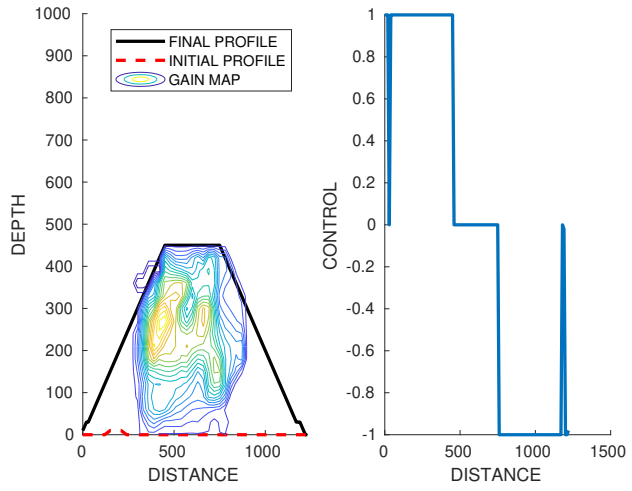

Figure B.11: 1D profile with infinite capacity - global optimization (HJB method)

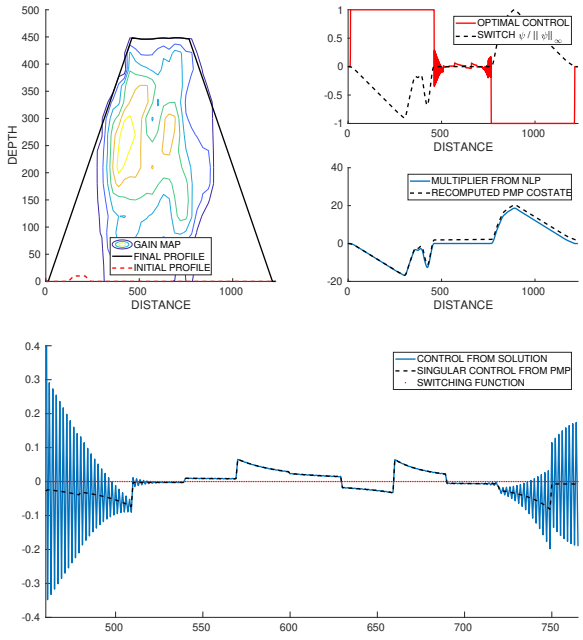

Figure B.12: 1D profile with infinite capacity - local optimization (direct method) and consistency with PMP optimality condition

Appendix B.2. FOP with infinite capacity and variable slope

Here we illustrate a case with a non-constant maximal slope κ. For this, we consider following arbitrary κ function:

$$\kappa(x,z) = \begin{cases} 0.5 & x \in [0, 330) \\ 1 & x \in [390, 960) \\ 5 & x \in [960, 1230] \end{cases} \tag{B.1}$$

We chose a piece-wise constant function so that the assumption in section 3 is satisfied almost everywhere. The solutions from the global and local optimizations are shown in Fig. B.13 and Fig. B.14 respectively. This time we obtain a control structure that includes all possible types of arcs: **Bang-Singular-Bang-Constrained**. The main difference compared to the constant slope case is that the optimal profile digs less ground on the right side region where the

gain is negative, as a steeper slope is allowed there. As for the previous examples we observe that the singular control and costate from the solution closely match their formal expressions from the PMP.

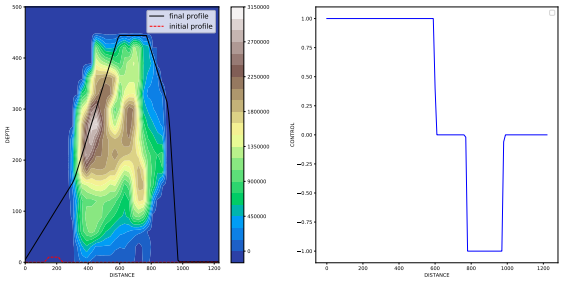

Figure B.13: 1D profile with infinite capacity and variable maximal slope - global optimization (HJB method)

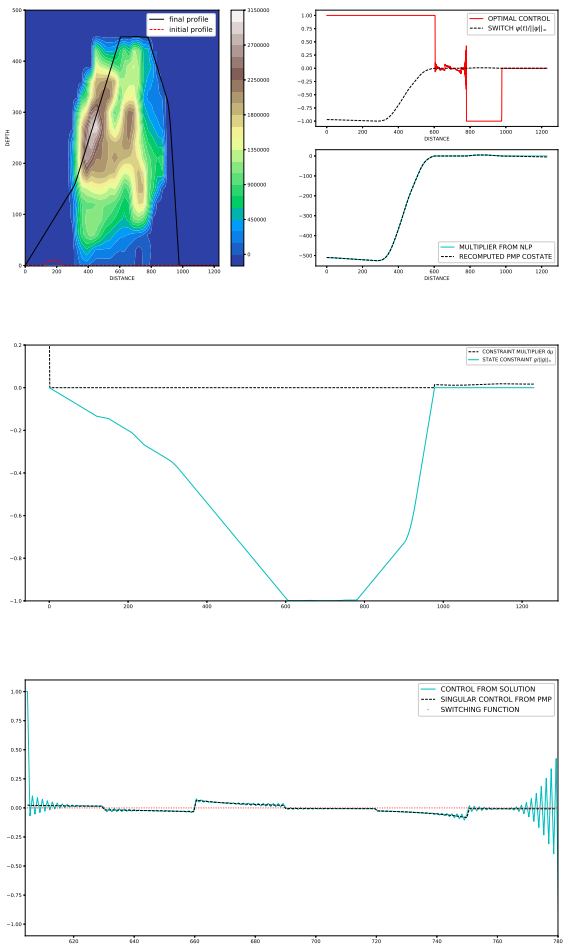

Figure B.14: 1D profile with infinite capacity and variable maximal slope - local optimization (direct method) with PMP optimality conditions